Enhancing dominant modes in nonstationary time series by means of the symbolic resonance analysis

Peter beim Graben[a)]
School of Psychology and Clinical Language Sciences, University of Reading, Reading RG6 6AH, United Kingdom

Heiner Drenhaus
Institute of Linguistics, University of Potsdam, Potsdam 14469, Germany

Eva Brehm
Interdisciplinary Center for European Languages, Free University Berlin, Berlin 14195, Germany

Bela Rhode
Institute of Linguistics, University of Potsdam, Potsdam 14469, Germany

Douglas Saddy
School of Psychology and Clinical Language Sciences, University of Reading, Reading RG6 6AH, United Kingdom

Stefan Frisch
Day-Care Clinic of Cognitive Neurology, University of Leipzig, Leipzig 04103, Germany and Max-Planck Institute for Human Cognitive and Brain Sciences, Leipzig 04103, Germany

(Received 11 April 2007; accepted 8 September 2007; published online 19 October 2007)

We present the symbolic resonance analysis (SRA) as a viable method for addressing the problem of enhancing a weakly dominant mode in a mixture of impulse responses obtained from a nonlinear dynamical system. We demonstrate this using results from a numerical simulation with Duffing oscillators in different domains of their parameter space, and by analyzing event-related brain potentials (ERPs) from a language processing experiment in German as a representative application. In this paradigm, the averaged ERPs exhibit an N400 followed by a sentence final negativity. Contemporary sentence processing models predict a late positivity (P600) as well. We show that the SRA is able to unveil the P600 evoked by the critical stimuli as a weakly dominant mode from the covering sentence final negativity. © *2007 American Institute of Physics*.
[DOI: 10.1063/1.2795434]

In addition to the characteristic temporal nonstationarity of impulse responses, dynamical systems exhibit another type of nonstationarity that is due to fluctuations or slow dynamics in parameter space. Both kinds are present in physiological measurements where, on the one hand, many realizations of noise-contaminated impulse responses have to be collected in order to increase the signal to noise ratio (SNR) by ensemble averaging, while, on the other hand, intertrial nonstationarity that is caused by changes in the system's control parameter weakens the SNR by damping the averaged impulse response and increasing its variance. In this paper, we treat different parameter-dependent impulse responses as modes that eventually contribute to the ensemble average, and show how weakly dominant modes can be enhanced by a symbolic time series analysis method, called symbolic resonance analysis. This approach takes advantage of the fact that the noise inherent in the data causes stochastic resonance effects in a threshold system. These resonances correspond to the phase transitions in a particular spin lattice that lead to a significant amplification of the SNR of the dominant mode. We present numerical simulations of the Duffing oscillator in two different regions of its parameter space. Finally, we apply the suggested method to event-related brain potentials (ERP) from a language processing experiment, where two antagonistic ERP components prevented an unambiguous interpretation of the analysis.

I. INTRODUCTION

Unlike in experimental physics,[1] astronomy,[2,3] or other physical sciences, where almost stationary time series of sufficient duration are often available, time series in the biological sciences are usually short and nonstationary.[4,5] This is especially the case in neuroscience where the reactions of neurons or neural networks upon particular stimuli can be regarded as impulse responses. Examples are, currents through single ion channels as measured in patch-clamp experiments,[6,7] receptor potentials,[8] local field potentials,[9] evoked or event-related brain potentials (ERP),[10–12] and functional magnetic imaging (fMRI) data[13,14] in psychophysics and cognitive neuroscience.

Although impulse response functions are also well known in the engineering and physical sciences, they are usually treated within the framework of linear system theory,

[a)]Electronic mail: p.r.beimgraben@reading.ac.uk

where their relationship to the transfer function describing the system's response to periodic forcing is mathematically given by the Laplace transform.[11] However, less is known about impulse responses of nonlinear dynamical systems.[15–17]

By definition, impulse response functions are transients and therefore temporally nonstationary. Nonlinear dynamical systems that depend on a control parameter additionally exhibit another kind of nonstationarity: For critical values, the system is very sensitive to small random perturbations or slow drifts in parameter space resulting in different qualitative behaviors when measurements are repeated many times. Yet, this is actually necessary in neurophysiological experiments in order to improve the signal to noise ratio (SNR) of the data by averaging over large ensembles of many time series.[10,18] Averaging across different impulse responses which are due to fluctuations or drifts in parameter space, however reduces the amplitudes and increases the variances of the data, thus diminishing the SNR. Therefore, a tradeoff between the impact of noise on short transient time series and the problem of intertrial nonstationarity is unavoidable in ensemble averages.

This can be nicely illustrated in the light of event-related brain potentials (ERPs) in psychophysics and cognitive neuroscience. ERPs are commonly regarded to be tiny impulse responses in the electroencephalogram (EEG) generated by neural networks that are time-locked to the perception or processing of stimuli and blended by the spontaneous EEG that reflects the ongoing, continuous activity of the brain.[10,18] As the typical ERP amplitude is in the range of $5-10\ \mu$V which is at least one order of magnitude smaller than the background EEG, one usually repeats the stimulus presentation between 30 and 1000 times per subject and averages across "epochs" that are time-locked to the stimulus. The single-subject ERPs obtained from 10 to 30 subjects are further averaged into the grand averages which display several peaks with distinct polarity, latency (the time of the maximal deflection), morphology, and topography. The conventional terminology takes all of these parameters into account and names ERP components according to their polarity and latency time, such as P300 (a positivity, 300 ms after stimulus onset), N400 (a negativity, 400 ms after stimulus onset), or P600 (a positivity, 600 ms after stimulus onset), all with rather long duration and broadly distributed over parietal recording sites at the scalp. The latter two components are related to language processing problems in the semantic and syntactic domain, respectively. The N400 is elicited by semantically odd sentence continuations such as in "he spread the warm bread with **socks**."[19] The P600, on the other hand, occurs in sentences like "the broker persuaded **to** sell the stock" where the critical stimulus "**to**" cannot be integrated into a syntactic representation of the sentence that has already been built up because "persuaded" is a transitive verb requiring a direct object (such as "the shareholder") instead of a sentence complement as indicated by "to."[20] For reviews on language processing ERP research, see Refs. 21–24.

Following Başar[11,12] and beim Graben *et al.*,[25] ERPs can be interpreted in the framework of dynamical system theory as follows: The measurable EEG maps the phase space of the brain onto a multivariate observable space such that single ERP epochs are represented by transient trajectories exploring this low-dimensional space that start from randomly distributed initial conditions, each one corresponding to one repetition of the experiment. These trajectories, which can be seen as impulse responses, depend on fluctuating or changing control parameters: First of all, in each ERP experiment one has to designate the control and the critical conditions which correspond to fixed domains in parameter space. Moreover, different subjects participating in an ERP experiment may employ different strategies to cope with the tasks.[26–28] These between-subject differences have to be taken into account when making the grand average analysis. Finally, when conducting an ERP experiment, each single subject may undergo slow changes in attention, habituation, learning, fatigue, etc.[29–32]

To discuss an example, Osterhout (Ref. 26, Exp. 2) investigated the processing of sentences of the kind "the boat sailed down the river **sank** during the storm" in comparison to sentences such as "the boat sailed down the river and **sank** during the storm." While the latter is syntactically normal, the former elicits a processing problem at the critical word (in bold) as it is not expected by the sentence context. Instead, a costly reanalysis is required to realize that "the boat sailed down the river" has to be analyzed as a reduced relative clause "the boat (that) sailed down the river." The sentence becomes completely acceptable after this revision. However, as the sentence appears to be syntactically anomalous, it also entails semantic interpretation problems. Therefore, a "biphasic" pattern of an N400, followed up by a P600 was observed in the grand average ERP. Yet, inspecting the single-subject averages revealed individual processing differences: one subject group, exhibiting only an N400, presumably pursued a semantic strategy, whereas another group which employed a syntactic strategy, produced the P600 in the ERP (for similar findings, see Refs. 27 and 28). This example does clearly demonstrate that impulse responses could spuriously superimpose in the average although they are due to different control parameters in the single trials. With respect to ERP analysis, the example is less problematic for the components with different latencies. Even worse is the case when components with similar spatio-temporal characteristics superimpose in the average.

For decomposing signals into independent sources, methods of blind source separation (BSS), such as principle component analysis (PCA, e.g., Ref. 33) or independent component analysis (ICA, e.g., Ref. 34) became recently popular for EEG/ERP analysis.[35–39] BSS techniques are devoted to solve the so-called cocktail-party problem where signals from different sources are blended to a noisy gossip. By recording this mixture from a multitude of sensors, BSS is able to reconstruct the original signals. However, the ICA model is comprised of four essential requirements:[40,41] (1) The source signals superimpose linearly and instantaneously, i.e., signal propagation times or convolutive mixing processes should be negligible. (2) The sources are spatially fixed and do not move (spatial stationarity). (3) The source signals are (maximally) temporally independent. (4) The sources have non-Gaussian distributions. These prerequisites

have to be fulfilled only weakly. Meinecke *et al.*,[42] e.g., showed that ICA successfully decomposes nonindependent but rather phase-synchronized signals; while Anemüller *et al.*[43] suggested complex ICA as a generalization that is able to cope with frequency-dependent superposition coefficients and convolutive mixing.

The separation of overlapping ERP components in averaged ERP signals by means of ICA has been demonstrated by Makeig *et al.*[44,45] Makeig *et al.*,[35] Jung *et al.*,[38] and Debener *et al.*[39] have suggested decomposing single-trial ERPs by concatenating the ERP epochs from all experimental conditions and then running ICA on these data streams obtained from each subject separately. However, this procedure is justified only when almost all ERP epochs consistently exhibit the same mixture of overlapping ERP components. Then, their concatenation will result in an almost stationary time series that can be subjected to the ICA algorithm. By contrast, in our case when one portion of ERP epochs contains one component and another portion contains another one (as in Osterhout[26]), the concatenation procedure would yield a signal lacking requirement (2), namely spatial stationarity. This can be illustrated by imagining a cocktail party where nonmoving guests start singing a canon. Although the sources are spatially fixed, their signals are not, they are moving around. In a similar way, the concatenation of differently behaving ERP epochs, where one portion contributes, e.g., a P600 while another portion contributes, e.g., an N400, provides a spatially nonstationary data stream. The applicability of ICA to such nonstationary data is at least questionable.

This paper addresses such issues of nonstationarity. In Sec. II, we model an ensemble of noisy data that comprises two different transient impulse responses occurring in different proportions. We show that the recently suggested symbolic resonance analysis (SRA) (Refs. 46–49) is not only able to detect the impulse response functions covered by additive noise, but moreover, that a prevalent impulse response function is significantly enhanced, even if it is only weakly dominant, thus improving the SNR of the data. In Sec. III, we apply the method to neurophysiological data from a language processing experiment, where two different components were intermingled in the averaged ERP, yet one as a weakly dominant mode. We conclude with a final discussion in Sec. IV.

II. THE SYMBOLIC RESONANCE ANALYSIS

A. Concepts

Our method, the symbolic resonance analysis (SRA), belongs to the wide class of symbolization (coarse-graining) methods that have been devised for the analysis of nonstationary time series.[4,25,50–55]

Let us assume that an ensemble of N measured time series $x_i(t)$ of duration T $(1 \le i \le N; 1 \le t \le T)$ is composed from K different impulse response functions $s_k(t)$ $(1 \le k \le K)$, each occurring N_k times, superimposed with i.i.d. white noise,

$$x_i(t) = s_{k_i}(t) + \xi_i(t), \tag{1}$$

where $k_i \in \{1,2,\ldots,K\}$ for $i \le N$ tells which impulse response is contained in the ith realization of the stochastic process with random component $\xi_i(t)$ $[\langle \xi_i(t) \rangle = 0$, $\langle \xi_i(t)^2 \rangle = \sigma^2$, $\langle \cdot \rangle$ denoting the ensemble average].

Since the components $s_k(t)$ contribute to the averaged impulse response,

$$r(t) = \frac{1}{N}\sum_{i=1}^{N} x_i(t) = \sum_{k=1}^{K} q_k s_k(t), \tag{2}$$

with the weight $q_k = N_k/N$, we call them modes of the averaged impulse response. The dominant mode $s_d(t)$ is that mode that is most often realized within the ensemble of time series, Eq. (1), with weight $q_d > q_k$ for all $k \ne d$. We call $s_d(t)$ weakly dominant if the dominant mode is present in about 60% of realizations.

Basically, the SRA relies upon the cooperative interplay between the noise and a nonlinear threshold crossing detector of a symbolic dynamics with three symbols.[46,56,57] The first step is a coarse-graining of the time series, Eq. (1), after choosing a certain threshold θ, according to

$$S_{it} = \begin{cases} a_0 & : \quad x_i(t) < -\theta \\ a_1 & : \quad |x_i(t)| \le \theta \\ a_2 & : \quad x_i(t) > \theta, \end{cases} \tag{3}$$

where $a_0 =$ "0", $a_1 =$ "1", $a_2 =$ "2" are the arbitrarily chosen symbols of the coarse-graining.

The symbolically encoded time series then form an array

$$\mathbf{E} = \begin{bmatrix} S_{11} & S_{12} & S_{13} & \cdots & S_{1T} \\ S_{21} & S_{22} & S_{23} & \cdots & S_{2T} \\ \vdots & \vdots & \vdots & \cdots & \vdots \\ S_{N1} & S_{N2} & S_{N3} & \cdots & S_{NT} \end{bmatrix} \tag{4}$$

of symbols S_{ij} comprising N rows (the number of realizations) and T columns (the number of sampling points in time).

From $\mathbf{E}$ the three-symbol distribution $(j = 0,1,2)$

$$p_j(t) = \frac{\#(a_j(t))}{N} \tag{5}$$

is determined. Here, $\#(\cdot)$ denotes the counting function applied to the symbol a_j at time t.

These symbol distributions are subjected to a spin-flip dynamics where the mean-fields of two competing Potts spins[58]

$$\begin{aligned} M_0(t) &= p_0(t) - p_1(t), \\ M_2(t) &= p_2(t) - p_1(t) \end{aligned} \tag{6}$$

try to flip the "undecided" between-threshold symbol "1" into either "0" or "2" leading to a distribution of only two symbols

$$p_0'(t) = \begin{cases} p_0(t) & : \quad M_2(t) > 0 \geq M_0(t) \\ p_0(t) + p_1(t) & : \quad M_2(t) \leq 0 < M_0(t) \\ p_0(t) + p_1(t)/2 & : \quad \text{otherwise}, \end{cases}$$
$$p_1'(t) = 1 - p_0'(t). \tag{7}$$

Thereby, the phase transitions of this symbolic dynamics considered as a $(1+1)$-dimensional Potts spin lattice[58] correspond to the instances of aperiodic stochastic resonance[59] in the threshold system.[56,57] Note that we use here a slightly modified definition of the mean-fields compared to that given in Ref. 46, Eq. (5), in order to highlight the competition between the "0"s and the "2"s for the "1"s.

According to Eq. (7), the transformed word statistics $p_j'(t)$ reflect the dominant mode $s_d(t)$ in the ensemble, Eq. (1), which causes one mean-field, either $M_0(t)$ or $M_2(t)$ to win the competition for the "1"s.

B. Simulations

In our simulations we studied the impulse response functions of the nonlinear Duffing oscillator[60] that has been suggested as a model for evoked brain potentials.[61] The system obeys the differential equation

$$\ddot{s} + \delta\dot{s} - \beta s - s^3 = 0 \tag{8}$$

with control parameters δ (damping) and β ("spring constant"). For $\delta > 0$, the system undergoes a pitchfork bifurcation from one stable fixed point $s^* = 0$ for $\beta < 0$ that destabilizes at $\beta = 0$ generating two stable fixed points $s^* = \pm\sqrt{\beta}$ for $\beta > 0$.[60]

For the sake of simplicity, we simulated Eq. (8) with only two different settings: (1) $\beta_1 = -1$ and (2) $\beta_2 = +0.1$, i.e., the attractors were $s^* = 0$ and $s^* = \pm 0.32$, while $\delta = 1$ has been kept constant during the simulations. Furthermore, we always used the same initial condition $(s, \dot{s}) = (1, 1)$ in order to avoid phase and therefore latency fluctuations.[62,63] The solutions $s_1(t)$, $s_2(t)$ of Eq. (8) for the different parameter settings were superimposed with zero-mean Gaussian white noise with different variances σ^2 according to Eq. (1). The ensembles of size $N = 500$ were generated with three mixture ratios $q = 0.6, 0.7$, and 0.8, where $s_1(t)$ was taken as the dominant mode. To this end, qN replicas of $s_1(t)$ and $(1-q)N$ replicas of $s_2(t)$ with random indices k_i entered the ensemble Eq. (1). Additionally, two "pure" ensembles consisting only of $s_1(t)$ $(q = 1)$ or $s_2(t)$ $(q = 0)$, respectively, superimposed with noise were created for the purpose of comparison.

Figure 1 displays the transient impulse responses $s_1(t)$ (solid line), $s_2(t)$ (dotted line), and the ensemble average $r(t)$, Eq. (2), (dashed line) for a noise intensity of $\sigma^2 = 0.6$. Additionally, the empirical standard deviation (dot-dashed line) of the ensemble, Eq. (1), is shown. The mixture ratio is $q = 0.6$ for Fig. 1(a), $q = 0.7$ for Fig. 1(b), and $q = 0.8$ for Fig. 1(c). Obviously, the averaged impulse response tends towards s_1 for increasing q from Figs. 1(a)–1(c).

For the SRA, the ensembles, Eq. (1), were subjected to the symbolic encoding, Eq. (3), with threshold $\theta = 0.35$ which is slightly larger than the height of the first local minimum of $s_1(t)$ around $t = 3$. Superimposed noise will therefore entail highly probable threshold crossing events, i.e., stochastic resonance, thus preparing this peak for evaluation. Employing Eq. (3) yielded the arrays, Eq. (4). Figure 2(a) presents a visualization for $\sigma^2 = 0.6, q = 0.8$, corresponding to Fig. 1(c) where black pixels denote "0," gray "1," and white "2."

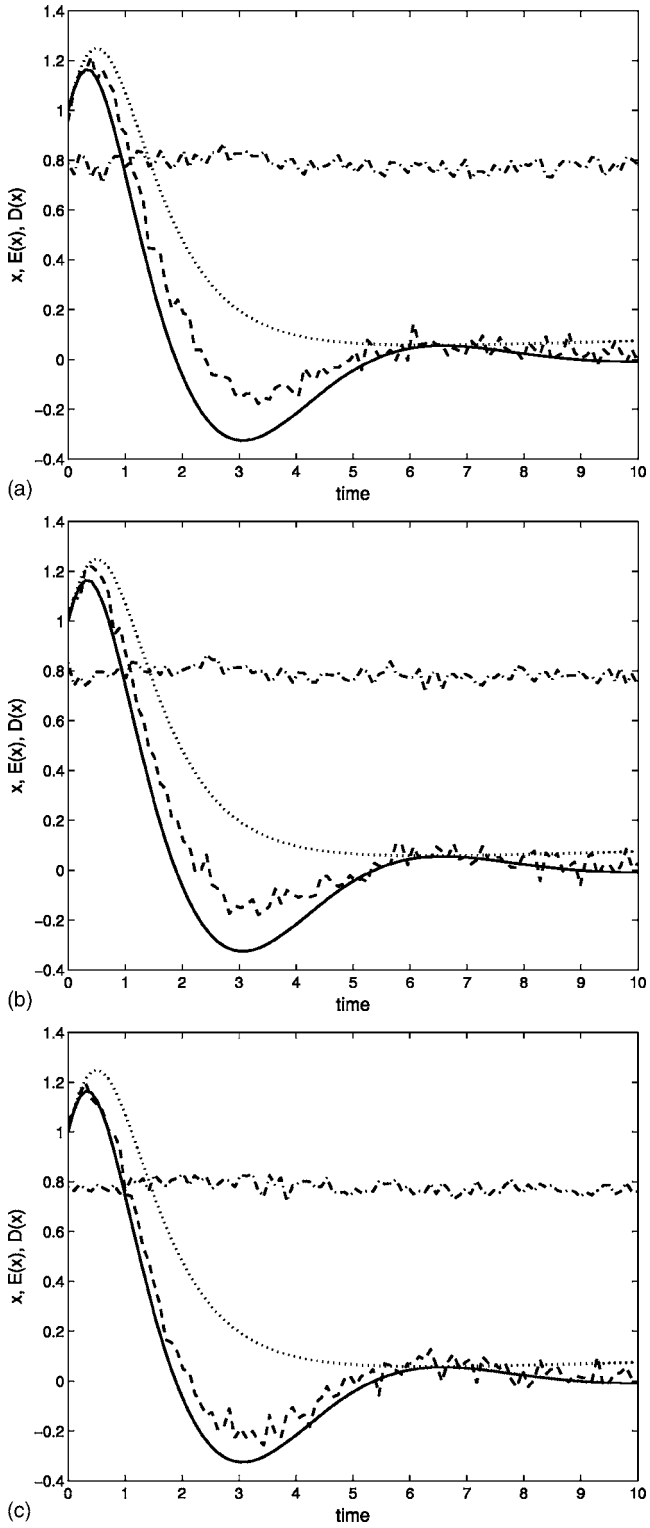

FIG. 1. Transient impulse responses $s_1(t)$ (solid line), $s_2(t)$ (dotted line) of the Duffing oscillator, Eq. (8), and the ensemble averages $r(t)$, Eq. (2), (dashed line) and their respective empirical standard deviations (dot-dashed line) from the mixtures, Eq. (1), with noise level $\sigma^2 = 0.6$ and mixture ratios (a) $q = 0.6$, (b) $q = 0.7$, (c) $q = 0.8$ of the dominant mode $s_1(t)$.

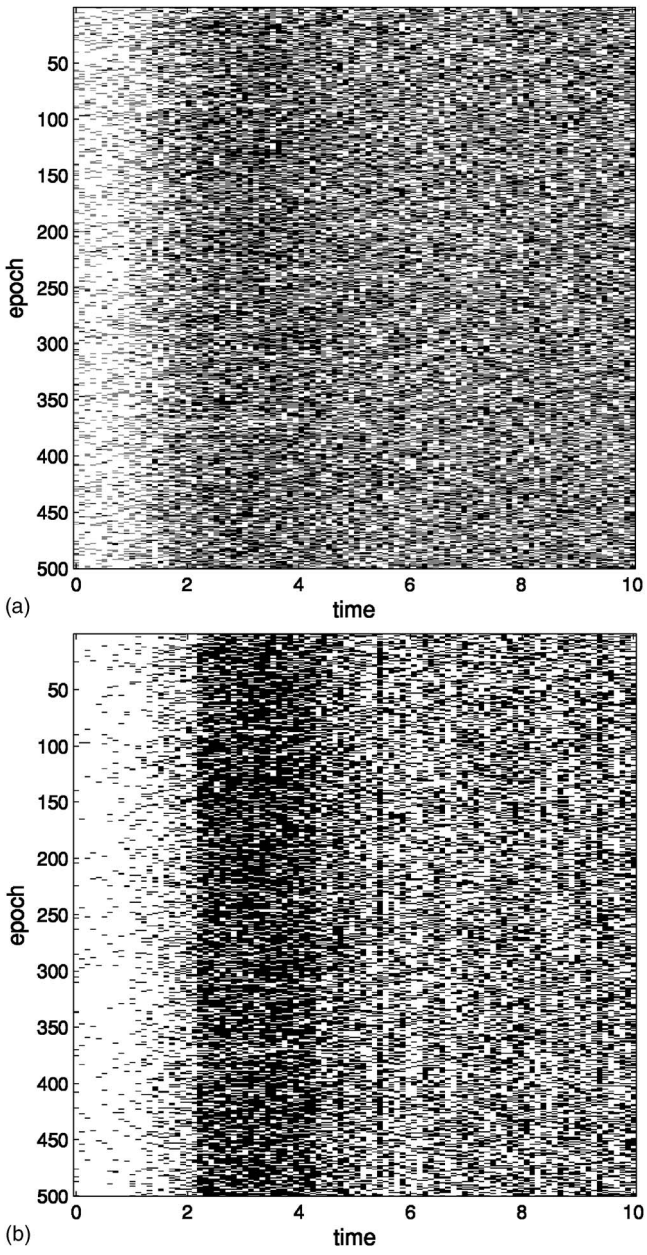

FIG. 2. Symbolic dynamics, Eq. (4), of (a) the symbolically encoded ensemble, Eq. (1), from Fig. 1(c) with $\sigma^2=0.6$, $q=0.8$. Black pixels denote "0," gray "1," and white "2." (b) The same ensemble after the mean-field transform, Eq. (7).

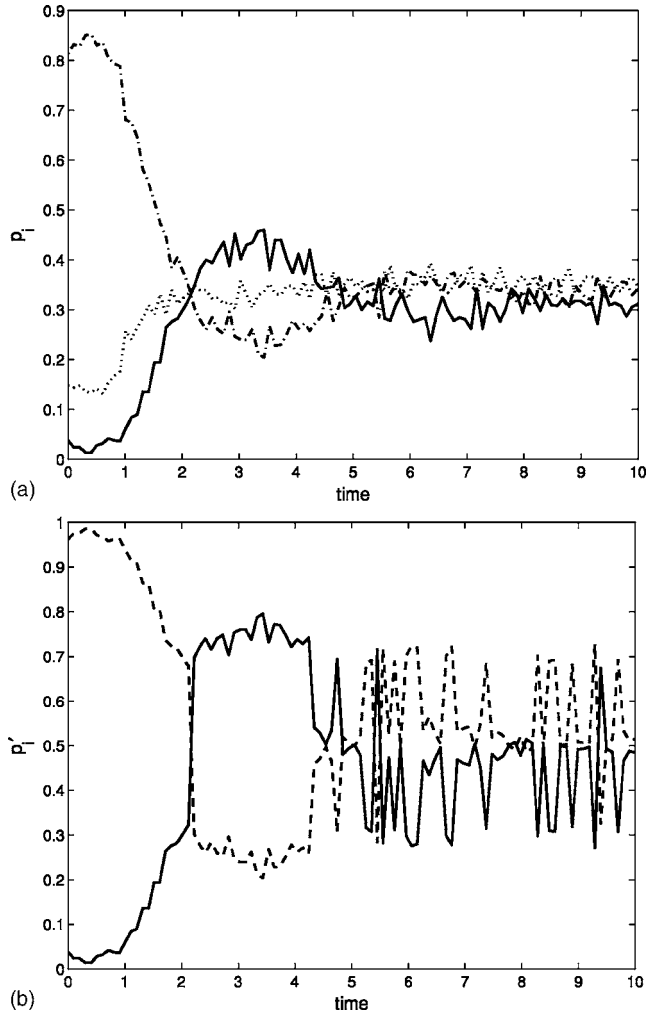

FIG. 3. Symbol distributions (word statistics) (a) $p_j(t)$ [Eq. (5)] as relative column frequencies from the ensemble, Eq. (1), shown in Fig. 2(a), solid line: $p_0(t)$; dotted line: $p_1(t)$; dashed line: $p_2(t)$. (b) $p'_j(t)$ after the mean-field transform, Eq. (7); solid line: $p'_0(t)$; dashed line: $p'_1(t)$ [cf. Fig. 2(b)].

(Such visualizations, introduced by beim Graben *et al.*,[25] are similar to the "ERP images" in the continuous signal range.[35,36])

The distribution of "0"s, "1"s, and "2"s [Eq. (5)] for the same simulation is plotted in Fig. 3(a).

Next, the three-symbol distribution, Eq. (5), is subjected to the mean-field transform, Eq. (7), regarding the symbolic dynamics, Eq. (4), as a $(1+1)$-dimensional Potts spin lattice.[58] The resulting distribution of two symbols "0" and "1" (formerly "2") obeys the normalization constraint $p'_0(t)+p'_1(t)=1$. For illustration, both functions are displayed in Fig. 3(b). Apparently, the three-symbol distribution $p_j(t)$ [Fig. 3(a)] is monotonically deviating from the uniform one around $t=3$ as there are more "0"s than "1"s and more "1"s than "2"s. Hence, the mean-field $M_0(t)$ won the competition and all "1"s were flipped into "0"s as shown in Fig. 3(b).

Although the mean-field transform, Eq. (7), applies directly to the word statistics, its action upon the symbolic dynamics can also be visualized as in Fig. 2(b). Here the spin-flip dynamics is easily recognized; all gray pixels have been converted either into white or black ones according to the competition between the mean-fields, Eq. (6). Again, the mean-field transform, Eq. (7), maps monotonic deviations from the uniform distribution onto nonuniform distributions. Conversely, all other distributions are mapped onto the uniform distribution of two symbols by flipping half of the "1"s into "0"s and the other half into "2"s. To create the visualization Fig. 2(b), the particular "1"s were chosen randomly from both halves. As a result, the local minimum of the dominant mode $s_1(t)$ around $t=3$ is represented by a black vertical stripe across all trials in the symbolization.

It is clear from the definition of the mean-field transform, Eq. (7), that all "1"s are flipped either into "0" or into "2" if there is one mean-field, either $M_0(t)$, or $M_2(t)$, winning the competition. This is especially the case, if a dominant mode prevails the ensemble, Eq. (1). In order to demonstrate

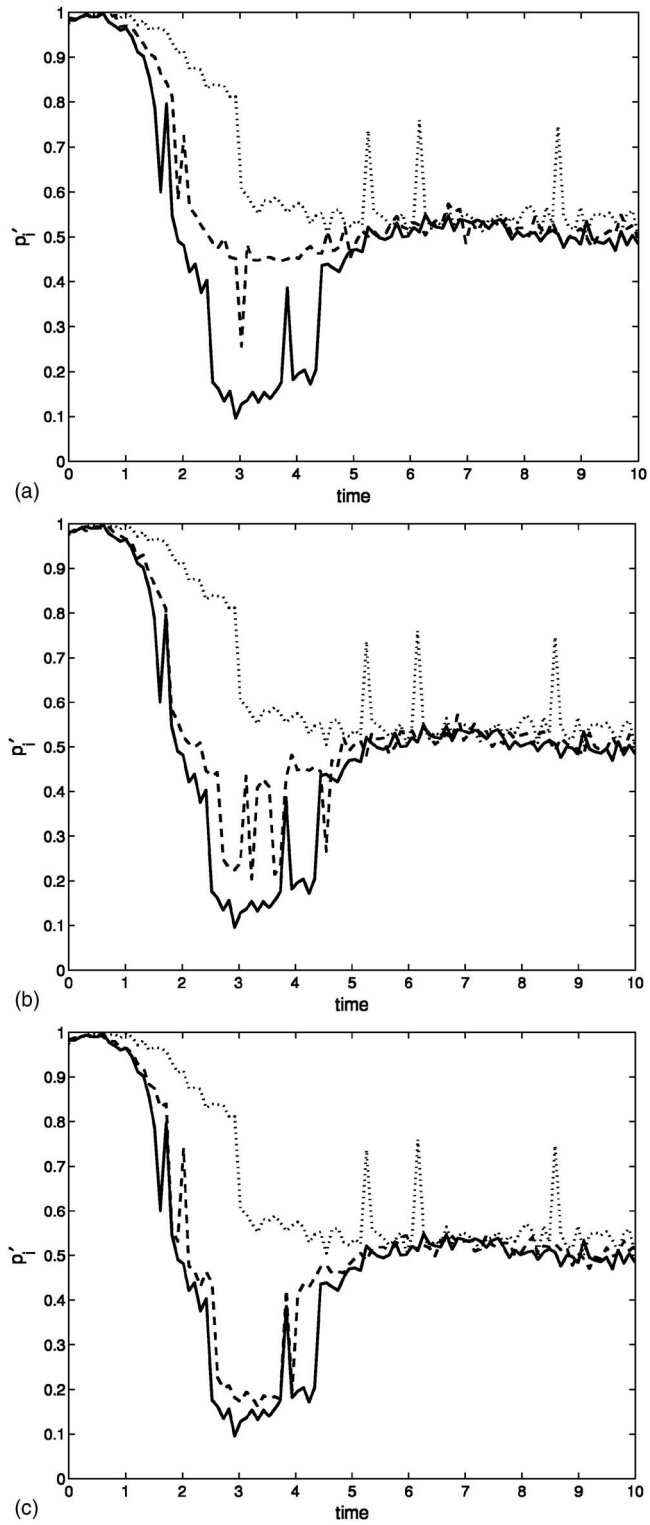

FIG. 4. The relative frequency $p_1'(t)$ (dashed line) after the mean-field transform Eq. (7) in comparison to the corresponding functions of the dominant mode $s_1(t)$ (solid line) and of the nondominant mode $s_2(t)$ (dotted line) of Eq. (8) for the ensemble, Eq. (1), with noise strength $\sigma^2=0.4$ for mixture ratios: (a) $q=0.6$, (b) $q=0.7$, (c) $q=0.8$.

this effect, we subsequently present results from our simulations with different mixture ratios, $q=0.6,0.7,0.8$ and different noise intensities, $\sigma^2=0.4,0.6,0.8$.

Figure 4 presents the mean-field transformed frequencies $p_1'(t)$ and both, the dominant mode $s_1(t)$ and the nondominant mode $s_2(t)$ of Eq. (8) after applying the SRA to their word statistics obeyed from the "pure" ensembles for the noise level $\sigma^2=0.4$ for comparison. For Fig. 4(a) $q=0.6$, Fig. 4(b) $q=0.7$, Fig. 4(c) $q=0.8$. Since the SRA has been optimized by choosing $\theta=0.35$, $p_1'(t)$ fits the corresponding probability obtained from the "pure" ensemble of $s_1(t)$ only for $q=0.8$ [Fig. 4(c)]. The correspondence for $q=0.6$ and $q=0.7$ [Figs. 4(a) and 4(b)] is rather poor, yet.

This changes, however, by increasing the noise intensity to $\sigma^2=0.6$ as shown in Fig. 5. As indicated by Fig. 5(a), even the lowest mixture ratio of $q=0.6$ provides a good detectability of this weakly dominant mode that further increases with higher q [Figs. 5(b) and 5(c)].

Nevertheless, the situation looks different again when the noise becomes too strong as shown in Fig. 6, where $\sigma^2=0.8$. In this case, the dominant mode remains hidden as long as $q=0.7$ or larger [Figs. 6(b) and 6(c)].

These results illustrate that even weakly dominant modes in a nonstationary ensemble of impulse responses can be enhanced by the SRA when additive noise and an optimally chosen encoding threshold cause a cooperative interplay between competing modes and hence stochastic resonance in the symbolic threshold system.

III. THE EXPERIMENT

Here we report results of an experiment testing particular language processing problems in German that are evoked by so-called negative polarity items (NPIs) such as adverbs like "ever" or phrases, like "not in the least" or "to lift a finger" that appear in sentences like "nobody lifted a finger to help me." These peculiar items have to occur in the semantic context of negation to be syntactically licensed.[64]

In an ERP experiment we tested negative polarity items in German such as *jemals* ("ever") that were correctly licensed by a negator *kein* ("no") against sentences without any negation. Table I displays examples for both conditions: In the correct condition (COR) a licensor is present whereas the structure is incorrect when there is no licensing negation (INC).

As predicted upon linguistic theory, previous studies on the processing of NPIs have shown that an unlicensed NPI elicits a biphasic N400/P600 response in the ERP.[49,65,66] Although Saddy *et al.*[67] reported only an N400 ERP effect for the processing of unlicensed NPIs, a *post-hoc* analysis of these data by our symbolic resonance analysis revealed also a significant P600.[49] We therefore expect a similar N400/P600 pattern in the ERPs of the present study. However, as can be seen in the sentence examples shown in Table I, the NPI *jemals* ("ever") is the next to last word followed by the concluding adjective [such as *traurig* ("sad")]. It is well-known from the literature that the terminating word of a sentence gives rise, under certain circumstances, to a large slow negative wave in the ERP, the sentence final negativity (SFN).[20,26,68] This component can override and hide a late P600 elicited by the preceding word.[21,69] This state of affairs is a concrete example of a weakly dominant mode within a mixture of impulse response functions.

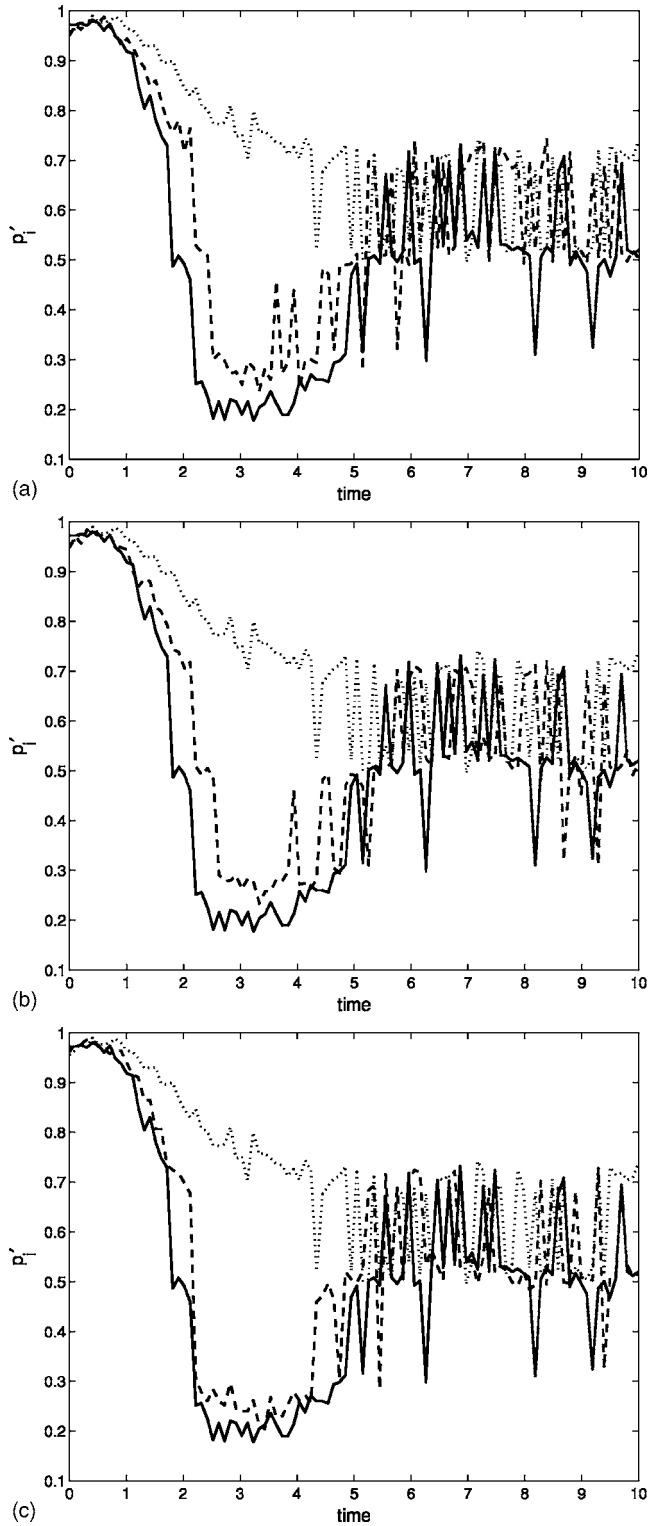

FIG. 5. The relative frequency $p_1'(t)$ (dashed line) after the mean-field transform, Eq. (7), in comparison to the corresponding functions of the dominant mode $s_1(t)$ (solid line) and of the nondominant mode $s_2(t)$ (dotted line) of Eq. (8) for the ensemble, Eq. (1), with noise strength $\sigma^2=0.6$ for mixture ratios: (a) $q=0.6$, (b) $q=0.7$, (c) $q=0.8$.

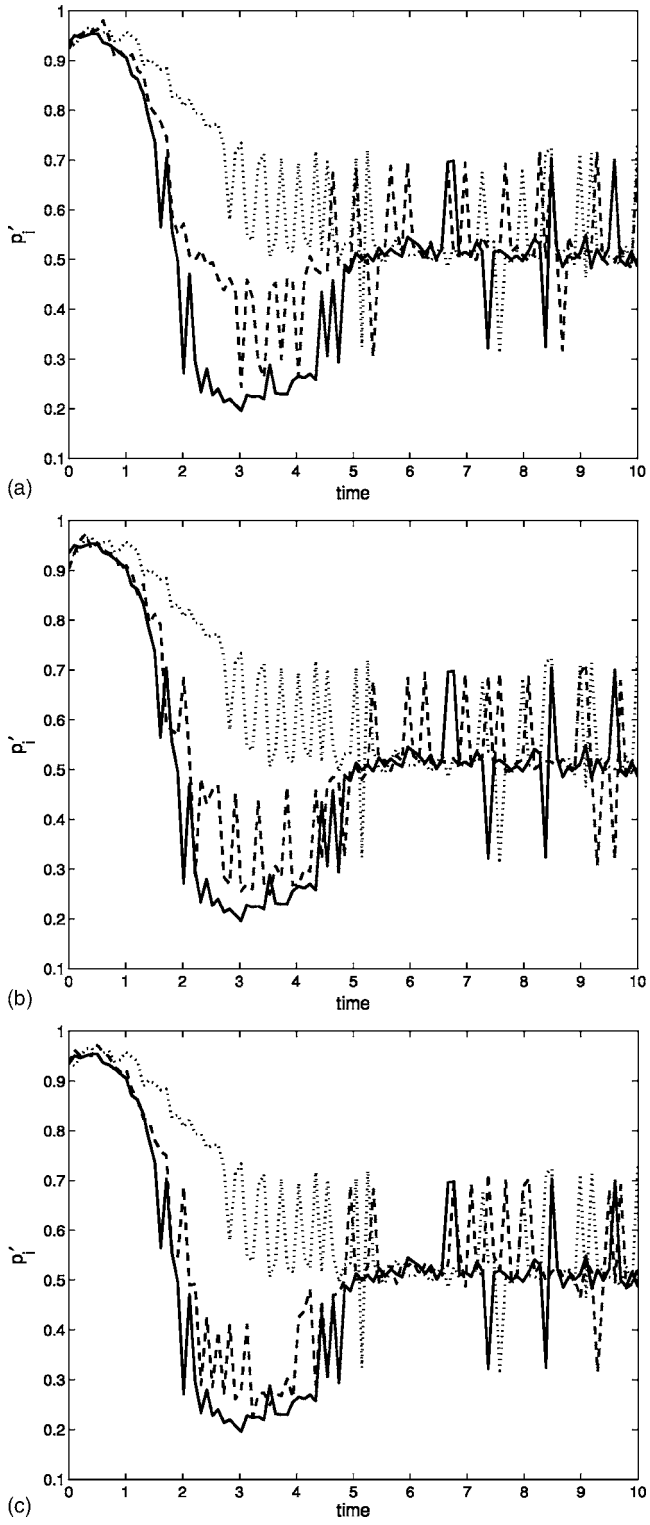

FIG. 6. The relative frequency $p_1'(t)$ (dashed line) after the mean-field transform, Eq. (7), in comparison to the corresponding functions of the dominant mode $s_1(t)$ (solid line) and of the nondominant mode $s_2(t)$ (dotted line) of Eq. (8) for the ensemble, Eq. (1), with noise strength $\sigma^2=0.8$ for mixture ratios: (a) $q=0.6$, (b) $q=0.7$, (c) $q=0.8$.

A. Materials and methods

Sixteen undergraduate students (mean age 19 years, nine females) from the University of Potsdam participated in the ERP study after giving informed consent. All were right-handed and had normal or corrected-to-normal vision.

Each subject read a total of 160 sentences in a pseudo-randomized order in which 80 critical sentences (40 per condition, see Table I) were intermixed with 80 related fillers.

TABLE I. Sample stimuli for each of the two experimental conditions. The critical words are printed in bold font.

Condition	Example			
COR	Kein Mann	war	**jemals**	traurig.
	No man	was	ever	sad.
INC	Ein Mann	war	**jemals**	traurig.
	A man	was	ever	sad.

All critical sentences consisted of main clauses. The negator appeared in the correct condition (COR) and the incorrect condition (INC) did not contain negation.

After a set of 20 training sentences (five in each of the critical conditions), all sentences were presented in the center of a 17 in. computer screen, with 400 ms (plus 100 ms blank screen resulting in 500 ms interstimulus interval) for the initial subject phrase and for each of the other words in isolation. 500 ms after the last word of each sentence, subjects had to judge its well-formedness within a maximal interval of 3000 ms by pressing one out of two buttons. 1000 ms after their response, the next trial began.

The EEG was recorded by means of 25 Ag/AgCl electrodes mounted according to the 10-20 system[70] with a sampling rate of 250 Hz (impedances <5 kΩ) and was referenced to the left mastoid (re-referenced to linked mastoids offline). EOG was monitored to control for eye-movement artifacts.

B. Data analysis

For the ERP analysis only artifact-free trials (520 and 511, for COR and INC, respectively, determined by visual inspection) with correct answers in the judgement task were selected. Epochs from −200 to 1400 ms relative to the presentation of the NPI were baseline corrected by subtracting the time average of the prestimulus interval. Mean ERPs were computed for each subject and condition and subsequently averaged into the grand averages. For statistical treatment, single-subject ERPs were time-averaged in two time windows: I from 300 to 500 ms according to the expected N400, and II from 800 to 1000 ms with respect to the expected late positivity in accordance with Drenhaus *et al.*[49,65,66] Repeated measures ANOVA for the expected ERPs (N400 in window I and P600 in window II) was performed with the factor VIOLATION for each of the three midline electrodes FZ, CZ, and PZ as well as for each of the following four lateral regions of interest (ROI): left-anterior (F7, F3, FC5), right-anterior (F8, F4, FC6), left-posterior (P7, P3, PO3), and right-posterior (P8, P4, PO4).

The EEG data have been preprocessed in the same way as for the voltage averaging, namely re-referenced and baseline aligned, before they entered the SRA as described in Sec. II.[46–49] The ith EEG epoch $x_{ik}^{(s,c)}(t)$ contributed by subject s, experimental condition c, and electrode k (t denotes the sampling point in time) is symbolically encoded into a string of three letters "0," "1," "2" by the encoding rule Eq. (3) with respect to a temporarily fixed voltage threshold θ. In a first step, all symbolic strings obtained in that way are collected into the grand epoch ensemble (GEE), Eq. (4). From these ensembles the relative frequency $p_i^{\mathrm{GEE}}(t)$ of the ith symbol at the instance of time t and across all epochs [Eq. (5)] is determined (where we omit condition and electrode indices subsequently; subject and epoch indices are already lost after forming the GEE).

These three-symbol distributions (the "polarity histograms" in the sense of Callaway and Halliday[29]) are then subjected to the mean-field transform, Eq. (7), where the algorithm detects peaks in the symbol distributions by reverting the between-threshold symbol "1" either into "0" or into "2." In the next step, an estimator of the signal to noise ratio (SNR) within two particular time windows $T=t_{\mathrm{off}}-t_{\mathrm{on}}$ was computed from the cylinder entropies[25] of the mean-field transformed word statistics

$$H(t) = -p_0'^{\mathrm{GEE}}(t)\log_2 p_0'^{\mathrm{GEE}}(t) - p_1'^{\mathrm{GEE}}(t)\log_2 p_1'^{\mathrm{GEE}}(t). \tag{9}$$

The SNR is then given by[46,62]

$$S = 0.5883\left(\frac{1}{1/T\Sigma_t H(t)} - 1\right), \tag{10}$$

measuring the deviation of the mean-field transformed symbol statistics from the uniform distribution. It is high if the frequency of either "0"s—indicating a negative peak—or "2"s—reflecting a positive peak—in the ensemble of ERP epochs is much larger then the frequency of its counterpart. On the other hand, the SNR estimator is low if neither "0"s, nor "2"s had won the competition for the "1"s in the mean-field transform. Therefore, the absence of any peak in the ERP is represented by an almost uniform distribution of the transformed symbols "0" and "1" (previously denoted as "2") exhibiting a low SNR. The SNR estimator is computed for the same time windows I: 300–500 ms and II: 800–1000 ms as for the ANOVA of the voltage ERPs.

Unlike in our simulations where the optimal threshold was explicitly given by the height of the peak of the dominant mode, there is no indication as to what such a threshold might be for experimental data. Therefore, a search in parameter space is necessary. To this end, the above mentioned procedure (choosing a threshold θ, followed by symbolic encoding, applying the mean-field transform, and determining the SNR) is repeated for a range of encoding thresholds starting with 2.5 to 12.0 μV in steps of 0.1 μV, such that to every threshold value θ a corresponding SNR value $S(\theta)$ is assigned. Plotting these functions for the experimental conditions c_1 vs c_2 yields characteristic curves that indicate the phenomenon of aperiodic SR in the threshold detector.[46–49,57] The optimal threshold $\theta^{\#}$ is then given by the maximal modulus of the difference of two resonance curves for two experimental conditions[48]

$$\theta^{\#} = \arg\max_{\theta} \left| S^{(c_1)}(\theta) - S^{(c_2)}(\theta) \right|. \tag{11}$$

These values are determined for every electrode separately. Using these thresholds, presented in Table II for the nine electrodes plotted in the figures, the GEEs obtained for the respective optimal thresholds are rearranged in order to create a new, optimal, GEE that contains for each electrode its particular optimally encoded symbol array. The statistics of

TABLE II. Optimal encoding thresholds (in μV) for the nine selected electrodes determined from the SNR of the two time windows I: 300–500 ms (N400) and II: 800–1000 ms (P600).

Window	F7	FZ	F8	P7	CZ	P8	PO3	PZ	PO4
I: 300–500 ms (N400)	4.5	7.1	6.3	6.6	5.6	6.9	7.3	6.5	3.4
II: 800–1000 ms (P600)	5.0	6.6	7.0	7.1	7.5	8.0	8.0	6.1	4.9

"0" (denoting negative voltage deflections) and "1" (denoting positive voltage deflections) [Eq. (5)] after the mean-field transform, Eq. (7), is comparable to the traditional ERP waveforms. Note that the relative frequencies of "0"s and "1"s sum to unity after the transform. Therefore, it is sufficient to plot only one of these functions for comparison between experimental conditions.

In order to employ repeated measures ANOVA, we need SRA results from each single subject. To this end, single-subject ensembles [Eq. (4)] are built like the optimal GEEs above. From these, the symbol distributions for subject s, $p_i^{(s)}(t)$ are derived according to Eq. (5). These single-subject distributions enter a modified mean-field transform, where the GEE distributions $p_i^{\mathrm{GEE}}(t)$ in Eq. (7) have to be replaced by their single-subject counterparts where the mean-fields of the optimal GEE act now collectively on the symbol distributions of each subject separately,

$$p_0'^{(s)}(t) = \begin{cases} p_0^{(s)}(t) & : \quad M_2(t) \geq 0 > M_0(t) \\ p_0^{(s)}(t) + p_1^{(s)}(t) & : \quad M_2(t) \leq 0 < M_0(t) \\ p_0^{(s)}(t) + p_1^{(s)}(t)/2 & : \quad \text{otherwise}, \end{cases}$$
$$p_1'^{(s)}(t) = 1 - p_0'^{(s)}(t). \tag{12}$$

The resulting mean-field transformed single-subject symbol distributions are time averaged in the same windows I and II as the mean ERPs and subsequently subjected to the ANOVA.

C. Results

1. Voltage averages

Figure 7 displays the grand average ERPs for the conditions COR (correctly licensed NPI) and INC (incorrect) at nine electrode sites.

The ungrammatical sentences INC elicit an N400. At times later than 800 ms the violation condition INC exhibits an anteriorly pronounced sentence final negativity shown at electrodes F7, FZ, and F8. At parietal sites (PO3, PZ, P04) the ERP for the INC condition is more positive compared to the COR condition. This suggests the expected confound of a very late P600 blended with the sentence final negativity in the epochs ensemble. The statistical analysis given in Table III reveals that the difference between both conditions is only significant at electrode FZ and the anterior ROIs where INC is more negative than COR. At parietal electrodes the superposition of the sentence final negativity with the P600 prevents any statistically reliable difference.

2. Symbolic resonance analysis

The SRA provides two sets of optimal thresholds (Table II) and their associated symbol distributions. We plot the probabilities $p_0'^{\mathrm{GEE}}(t)$ which denote resonant threshold crossing events with negative polarity obtained for the optimal thresholds from the N400 window I for both conditions COR and INC in Fig. 8. Correspondingly, Fig. 9 shows the frequencies $p_1'^{\mathrm{GEE}}(t)$, i.e., the probabilities to observe resonant threshold crossing events with positive polarity (originally encoded as "2") for the optimal thresholds from the P600 window II for both conditions COR and INC. Note that baseline problems, apparently present in the ERP voltage averages in Fig. 7, are suppressed by the SRA (Figs. 8 and 9) because these fluctuations do not give rise to stochastic resonance effects in the threshold ranges of the proper ERP components.

The N400 is highly amplified by the SRA analysis. This is also reflected by the results of the ANOVA applied to the mean-field filtered symbol distributions (Table IV).

More interesting, however, are the distributions of the mean-field transformed "1"s optimized for the late time window II. The COR condition contributed only a small number of trials with positive polarity (around 0.25 at electrodes P8, PO3, PO4) thus indicating that the "0"s (resonant negative voltages) won the competition for the "1"s against the "2"s.

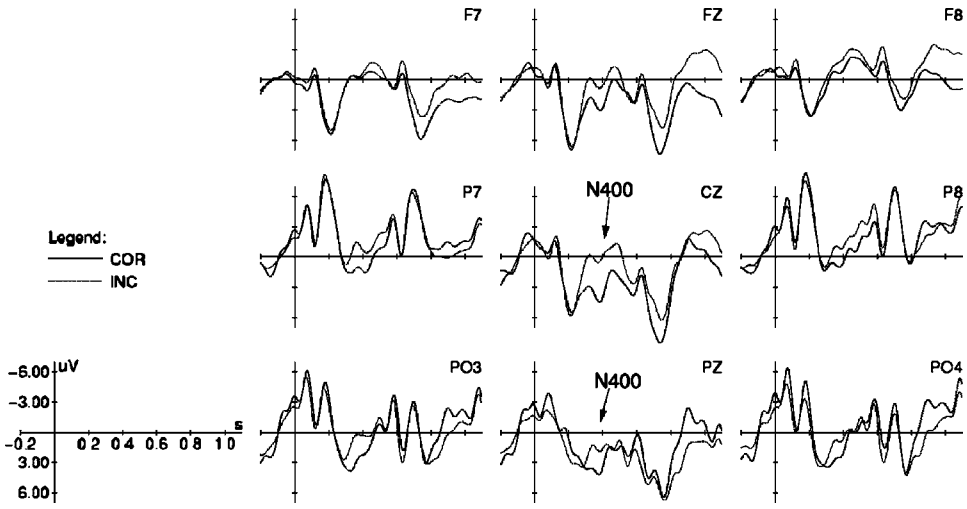

FIG. 7. ERP voltage averages for the conditions (COR) (bold line) and (INC) (thin line) at nine electrodes. Time onset of the critical stimulus (the NPI) at 0 s. The N400 ERP component is indicated by the arrows. Waveforms are filtered with a 10 Hz low-pass filter for better visibility. According to an electrophysiological convention, negativity is plotted upwards.

TABLE III. Results of a repeated measures ANOVA for the mean ERPs. "SFN" stands for an effect due to the sentence final negativity.

	Window I: 300–500 ms		Window II: 800–1000 ms	
	F	*p*	*F*	*p*
Midline				
VIOLATION	19.57	<0.001	<1	n.s.
VIOLATION × ELECTRODE	1.8	n.s.	12.14	<0.001
FZ	4.56	<0.05	8.17	<0.05 (SFN)
CZ	19.54	<0.001	<1	n.s.
PZ	3.22	n.s.	3.26	n.s.
Lateral				
VIOLATION	13.37	<0.01	<1	n.s.
VIOLATION × REGION	<1	n.s.	21.22	<0.001
VIOLATION × HEMISPHERE	<1	n.s.	<1	n.s.
VIOLATION × REGION × HEMISPHERE	4.78	<0.05	<1	n.s.
Left-anterior	2.59	n.s.	12.28	<0.01 (SFN)
Right-anterior	6.54	<0.05	9.24	<0.01 (SFN)
Left-posterior	29.87	<0.0001	1.29	n.s.
Right-posterior	9.78	<0.01	1.69	n.s.

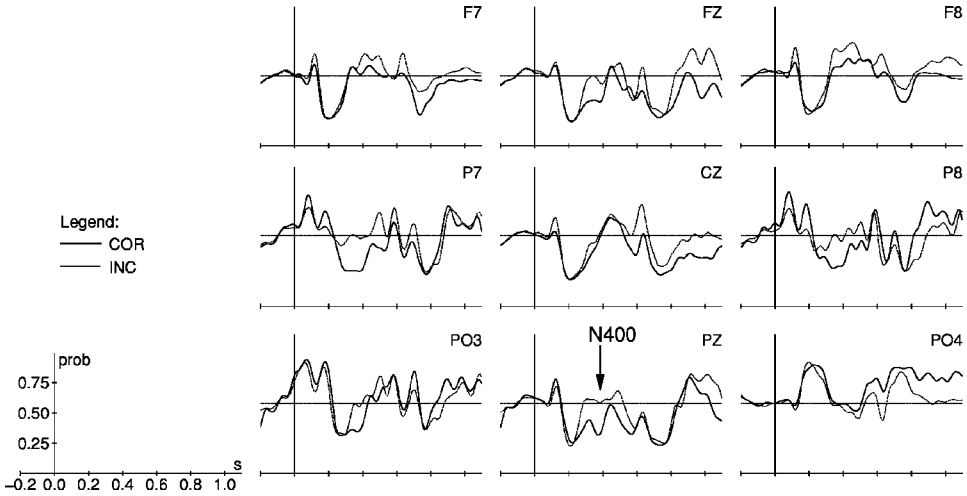

FIG. 8. Relative frequencies of trials with beyond-threshold negative polarity ("0"s) obtained for the respective optimal encoding thresholds of the nine selected electrodes (see Table II) after mean-field transform. Bold line: correct condition (COR); thin line: incorrect condition (INC). The N400 ERP component is indicated by the arrows. Waveforms are filtered with a 10 Hz low-pass filter for better visibility.

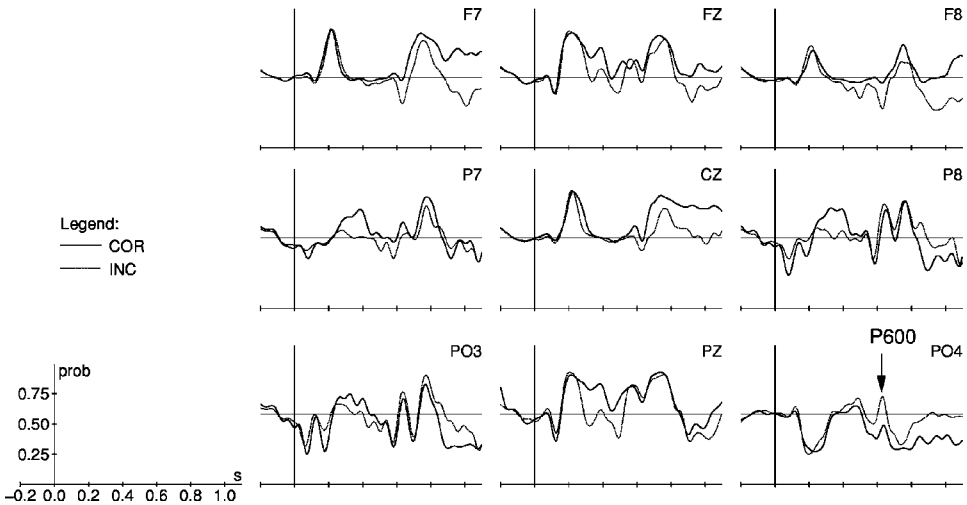

FIG. 9. Relative frequencies of trials with beyond-threshold positive polarity ("1"s) obtained for the respective optimal encoding thresholds of the nine selected electrodes (see Table II) after mean-field transform. Bold line: correct condition (COR); thin line: incorrect condition (INC). The P600 ERP component is indicated by the arrows. Waveforms are filtered with a 10 Hz low-pass filter for better visibility.

TABLE IV. Results of a repeated measures ANOVA for the distributions of the symbol "0" obtained from the SRA for the optimal thresholds for window I and for the distributions of the symbol "1" obtained from the SRA for the optimal thresholds for window II. "SFN" stands for an effect due to the sentence final negativity while "P600" denotes an effect due to the P600.

	Window I: 300–500 ms		Window II: 800–1000 ms	
	F	*p*	*F*	*p*
Midline				
VIOLATION	63.82	<0.0001	47.65	<0.0001 (SFN)
VIOLATION × ELECTRODE	59.20	<0.0001	8.59	<0.01
FZ	23.87	<0.001	36.52	<0.0001 (SFN)
CZ	8.7	<0.05	58.70	<0.0001 (SFN)
PZ	117.9	<0.0001	22.96	<0.001 (SFN)
Lateral				
VIOLATION	65.78	<0.0001	1.95	n.s.
VIOLATION × REGION	<1	n.s.	170.16	<0.0001
VIOLATION × HEMISPHERE	<1	n.s.	19.4	<0.001
VIOLATION × REGION × HEMISPHERE	11.42	<0.01	4.22	0.06
Left-anterior	21.71	<0.001	67.13	<0.0001 (SFN)
Right-anterior	35.86	<0.0001	50.9	<0.0001 (SFN)
Left-posterior	78.71	<0.0001	7.14	<0.05 (P600)
Right-posterior	66.77	<0.0001	55.41	<0.0001 (P600)

On the other hand, this competition ended in a draw for the unacceptable INC condition. After the transform there were almost the same numbers of "0"s and "1"s at channels P8 and PO3 meaning that the original distribution of "0"s was not strong enough to flip the "1"s into "0"s, while the "2"s obviously won the competition at PO4 (see Fig. 9). The symbol distributions of the SRA therefore allow us to conclude that the sentence final negativity was not present in the majority of EEG epochs and that a confounding P600 prevented it from winning the competition of the spin-flip dynamics. Table IV confirms this finding by means of the statistical analysis. The sentence final negativity clearly dominates at all midline electrodes FZ, CZ, and PZ, as well as at anterior ROIs, while the P600, the weakly dominant mode, is stronger at posterior ROIs.

IV. DISCUSSION

In this paper, we demonstrated through numerical simulations and via experimental data how a recently developed data analysis technique, the SRA,[46–49] is able to enhance dominant modes in ensembles of noisy time series that are nonstationary in two different aspects: first, temporal nonstationarity as is characteristic for impulse responses, and second, nonstationarity across the trial dimension that is due to fluctuations or gradual variations in the system's control parameters.

For the numerical simulations we investigated the impulse responses of the Duffing oscillator[60,61] in two parameter domains, this side of and beyond the pitchfork bifurcation. The system was contaminated with observational noise facilitating the occurrence of stochastic resonance in a symbolic dynamics with three symbols. For a critical noise level, the dominant mode became detectable even for a mixture ratio of 60%.

On the other hand, we used a language processing experiment, where two different modes in the voltage average were elicited, as a representative ERP paradigm: the P600 found in previous ERP studies with similar experimental manipulations,[49,65,66] and, the sentence final negativity,[26,71] evoked by the last word of the stimulus sentences following the critical word. An interaction of a late positivity and the sentence final negativity can arise if they are elicited by adjacent items.[21,72] They may also interact when they are elicited by one and the same item (i.e., critical item in sentence final position[69]). In the present experiment, the problem seems to be that the P600 effect on the penultimate word is particularly late, thus reaching into the rather early negativity effect on the sentence final element.

By applying the SRA to the data of the present experiment, we revealed the superposition of the late positivity related to the processing of the critical stimuli, namely the negative polarity items, with the sentence final negativity evoked by the concluding word. The SRA showed that this superposition was due to differences in the intertrial coherences. Almost one half of the ERP epochs contributed to the late positivity while the other half contributed to the sentence final negativity. We found that the late positivity was a weakly dominant mode at right-parietal electrodes in the optimal encoding.

Our results are consistent with the interpretation of ERPs in terms of dynamical system theory[11,12] and experimental findings on single-trial variability in the ERP (Refs. 30–32 and 73–76) which can be seen as motion in parameter space. Especially, changes in the ERP that are related to habituation or learning would correspond to drifting control parameters.

Beyond the application presented here, the SRA could also be of significance for the analysis of any ensemble of noisy and nonstationary time series which are time-locked to

certain events. This is particularly the case for ion currents obtained from patch-clamp measurements,[6,7] receptor potentials,[8] local field potentials,[9] functional magnetic imaging,[13,14] or even ERPs—especially for clinical applications where inhomogeneous distributions of components across trials are to be expected such as for aphasics or children with language acquisition impairments.

ACKNOWLEDGMENTS

We gratefully acknowledge helpful discussions with Leticia Pablos Robles, Slawomir Nasuto, Jürgen Kurths, and Angela Friederici. This work has been partly supported by the Deutsche Forschungsgemeinschaft within the research group on "Conflicting Rules in Cognitive Systems" (Grant No. FOR 375/1-4 to D.S.).

[1] D. S. Broomhead and G. P. King, Physica D **20**, 217 (1986).
[2] J. Kurths and H. Herzel, Physica D **25**, 165 (1987).
[3] A. Hempelmann and J. Kurths, Ann. N.Y. Acad. Sci. **232**, 356 (1990).
[4] J. J. Żebrowski, W. Popławska, R. Baranowski, and T. Buchner, Acta Phys. Pol. B **30**, 2547 (1999).
[5] J. J. Żebrowski, R. Baranowski, and A. Przybylski, Acta Phys. Pol. B **34**, 3703 (2003).
[6] F. A. Edwards, A. Konnerth, B. Sakmann, and T.Takahashi, Pfluegers Arch. **414**, 600 (1989).
[7] A. Verkhratsky, O. A. Krishtal, and O. H. Petersen, Pfluegers Arch. **453**, 233 (2006).
[8] C. C. Hunt and R. S. Wilkinson, J. Physiol. (London) **302**, 241 (1980).
[9] N. K. Logothetis, J. Pauls, M. Augath, T. Trinath, and A. Oeltermann, Nature (London) **412**, 150 (2001).
[10] D. Regan, *Evoked Potentials in Psychology, Sensory, Physiology and Clinical Medicine* (Chapman and Hall, London, 1972).
[11] E. Başar, *EEG-Brain Dynamics. Relations Between EEG and Brain Evoked Potentials* (Elsevier/North Holland Biomedical, Amsterdam, 1980).
[12] E. Başar, *Brain Function and Oscillations*, Springer Series in Synergetics (Springer, Berlin, 1998), Vol. I.
[13] R. L. Buckner, J. Goodman, M. Burock, M. Rotte, W. Koutstaal, D. Schacter, B. Rosen, and A. M. Dale, Neuron **20**, 285 (1998).
[14] K. J. Friston, P. Fletcher, O. Josephs, A. Holmes, M. D. Rugg, and R. Turner, Neuroimage **7**, 30 (1998).
[15] R. J. P. de Figueiredo, "Generalized nonlinear impulse response and nonlinear convolution in a reproducing kernel Hilbert space F," Workshop on Information Theory and Applications, University of California, San Diego (2006).
[16] G. Keep, M. H. Pesaran, and S. M. Potter, J. Econometr. **74**, 119 (1996).
[17] S. M. Potter, J. Econ. Dyn. Control **24**, 1425 (2000).
[18] *Electroencephalography: Basic Principles, Clinical Applications, and Related Fields*, edited by E. Niedermeyer and F. H. L. da Silva (Lippincott Williams and Wilkins, Baltimore, 1999).
[19] M. Kutas and S. A. Hillyard, Science **207**, 203 (1980).
[20] L. Osterhout and P. J. Holcomb, J. Mem. Lang. **31**, 785 (1992).
[21] M. Kutas and C. K. van Petten, in *Handbook of Psycholinguistics*, edited by M. A. Gernsbacher (Academic, San Diego, 1994), pp. 83–133.
[22] L. Osterhout and P. J. Holcomb, in *Electrophysiology of Mind: Event-Related Brain Potentials and Cognition*, edited by M. G. H. Coles and M. D. Rugg (Oxford University Press, Oxford, 1995), Chap. 6.
[23] L. Osterhout, J. McLaughlin, and M. Berwick, Trends Cogn. Sci. **1**, 203 (1997).
[24] Y. Grodzinsky and A. D. Friederici, Curr. Opin. Neurobiol. **16**, 240 (2006).
[25] P. b. Graben, D. Saddy, M. Schlesewsky, and J. Kurths, Phys. Rev. E **62**, 5518 (2000).
[26] L. Osterhout, Brain Lang **59**, 494 (1997).
[27] A. D. Friederici, K. Steinhauer, A. Mecklinger, and M. Meyer, Biol. Psychol. **47**, 193 (1998).
[28] S. H. Vos, T. C. Gunter, H. Schriefers, and A. D. Friederici, Lang. Cognit. Processes **16**, 65 (2001).
[29] E. Callaway and R. A. Halliday, Electroencephalogr. Clin. Neurophysiol. **34**, 125 (1973).
[30] T. Gasser, J. Möcks, and R. Verleger, Electroencephalogr. Clin. Neurophysiol. **55**, 717 (1983).
[31] J. Möcks, T. Gasser, and P. D. Tuan, Electroencephalogr. Clin. Neurophysiol. **57**, 571 (1984).
[32] R. Q. Quiroga and E. L. J. M. van Luijtelaar, Int. J. Psychophysiol **43**, 141 (2002).
[33] A. D. Friederici, A. Mecklinger, K. M. Spencer, K. Steinhauer, and E. Donchin, Brain Res. Cognit. Brain Res. **11**, 305 (2001).
[34] A. Hyvärinen and E. Oja, Neural Networks **13**, 411 (2000).
[35] S. Makeig, M. Westerfield, T.-P. Jung, S. Enghoff, J. Townsend, E. Courchesne, and T. J. Sejnowski, Science **295**, 690 (2002).
[36] A. Delorme and S. Makeig, J. Neurosci. Methods **134**, 9 (2004).
[37] R. Vigário, V. Jousmäki, M. Hämäläinen, R. Hari, and E. Oja, in *Advances in Neural Information Processing Systems* (MIT Press, Cambridge, 1997), Vol. 10, pp. 229–235.
[38] T.-P. Jung, S. Makeig, M. Westerfield, J. Townsend, E. Courchesne, and T. J. Sejnowski, Hum. Brain Mapp **14**, 166 (2001).
[39] S. Debener, S. Makeig, A. Delorme, and A. K. Engel, Brain Res. Cognit. Brain Res. **22**, 309 (2005).
[40] S. Makeig, M. Westerfield, T.-P. Jung, J. Covington, J. Townsend, T. J. Sejnowsky, and E. Courchesne, J. Neurosci. **19**, 2665 (1999).
[41] T.-P. Jung, S. Makeig, M. J. McKeown, A. J. Bell, T.-W. Lee, and T. J. Sejnowski, Proc. IEEE **89**, 1107 (2001).
[42] F. C. Meinecke, A. Ziehe, J. Kurths, and K.-R. Müller, Phys. Rev. Lett. **94**, 084102 (2005).
[43] J. Anemüller, T. J. Sejnowski, and S. Makeig, Neural Networks **16**, 1311 (2003).
[44] S. Makeig, A. J. Bell, T.-P. Jung, and T. J. Sejnowski, in *Advances in Neural Information Processing Systems*, edited by D. Touretzky, M. Mozer, and M. Hasselmo (MIT Press, Cambridge, 1996), Vol. 8, pp. 145–151.
[45] S. Makeig, T.-P. Jung, A. J. Bell, D. Ghahremani, and T. J. Sejnowski, Proc. Natl. Acad. Sci. U.S.A. **94**, 10979 (1997).
[46] P. b. Graben and J. Kurths, Phys. Rev. Lett. **90**, 100602 (2003).
[47] S. Frisch and P. beim Graben, Brain Res. Cognit. Brain Res. **24**, 476 (2005).
[48] P. b. Graben, S. Frisch, A. Fink, D. Saddy, and J. Kurths, Phys. Rev. E **72**, 051916 (2005).
[49] H. Drenhaus, P. beim Graben, D. Saddy, and S. Frisch, Brain Lang **96**, 255 (2006).
[50] M. Paluš, Biol. Cybern. **75**, 389 (1996).
[51] M. Paluš, V. Komárek, Z. Hrncír, and T. Procházka, Theory Biosci. **118**, 179 (1999).
[52] T. Buchner and J. J. Żebrowski, Phys. Rev. E **60**, 3973 (1999).
[53] M. Paluš, V. Komárek, T. Procházka, Z. Hrncír, and K. Tterbová, IEEE Eng. Med. Biol. Mag. **20**, 65 (2001).
[54] C. S. Daw, C. E. A. Finney, and E. R. Tracy, Rev. Sci. Instrum. **74**, 915 (2003).
[55] C. Piccardi, Chaos **16**, 043115 (2006).
[56] F. Moss, D. Pierson, and D. O'Gorman, Int. J. Bifurcation Chaos Appl. Sci. Eng. **4**, 1383 (1994).
[57] Z. Gingl, L. B. Kiss, and F. Moss, Europhys. Lett. **29**, 191 (1995).
[58] F. Y. Wu, Rev. Mod. Phys. **54**, 235 (1982).
[59] J. J. Collins, C. C. Chow, A. C. Capela, and T. T. Imhoff, Phys. Rev. E **54**, 5575 (1996).
[60] J. Guckenheimer and P. Holmes, *Nonlinear Oscillations, Dynamical Systems, and Bifurcations of Vector Fields*, in Springer Series of Appl. Math. Sciences (Springer, New York, 1983), Vol. 42.
[61] R. Srebro, Electroencephalogr. Clin. Neurophysiol. **96**, 561 (1995).
[62] P. b. Graben, Phys. Rev. E **64**, 051104 (2001).
[63] A. Puce, S. F. Berkovic, P. J. Cadusch, and P. F. Bladin, Electroencephalogr. Clin. Neurophysiol. **92**, 352 (1994).
[64] L. Horn, in *Negation and Polarity: Syntax and Semantics*, edited by D. Forget, P. Hirschbhler, F. Martinon, and M.-L. Rivero (John Benjamins, Amsterdam, 1997), pp. 157–182.
[65] H. Drenhaus, D. Saddy, and S. Frisch, in *Pre-Proceedings of the International Conference on Linguistic Evidence*, edited by S. Kepser and M. Reis (University Tübigen, Tübingen, 2004), pp. 41–46.
[66] H. Drenhaus, S. Frisch, and D. Saddy, in *Linguistic Evidence-Empirical, Theoretical, and Computational Perspectives*, Studies in Generative Grammar, edited by S. Kepser and M. Reis (Mouton de Gruyter, Berlin, 2005), Vol. 85, pp. 145–164.
[67] D. Saddy, H. Drenhaus, and S. Frisch, Brain Lang **90**, 495 (2004).
[68] L. Osterhout and P. J. Holcomb, Lang. Cognit. Processes **8**, 413 (1993).

[69]S. Frisch, *Verb-Argument-Struktur, Kasus und Thematische Interpretation beim Sprachverstehen*, MPI Series in Cognitive Neuroscience (MPI of Cognitive Neuroscience, Leipzig, 2000), p. 12.
[70]F. Sharbrough, G.-E. Chartrian, R. P. Lesser, H. Lüders, M. Nuwer, and T. W. Picton, J. Clin. Neurophysiol. **8**, 200 (1995).
[71]A. D. Friederici and S. Frisch, J. Mem. Lang. **43**, 476 (2000).
[72]M. G. Woldorff, Psychophysiology **30**, 98 (1993).
[73]R. Coppola, R. Tabor, and M. S. Buchsbaum, Electroencephalogr. Clin. Neurophysiol. **44**, 214 (1978).
[74]B. I. Turetsky, J. Raz, and G. Fein, Psychophysiology **26**, 700 (1989).
[75]A. Salajegheh, A. Link, C. Elster, M. Burghoff, T. Sander, L. Trahms, and D. Poeppel, Neuroimage **23**, 288 (2004).
[76]M. Atienza, J. L. Cantero, and R. Quian Quiroga, Neuroimage **26**, 628 (2005).